Energetics, conformation, and recognition of DNA duplexes containing a major adduct of an anticancer azolato-bridged dinuclear Pt^{II} complex

Jarmila Mlcouskova [a,b], Jaroslav Malina [b], Vojtech Novohradsky [a,b], Jana Kasparkova [a,b], Seiji Komeda [c], Viktor Brabec [b,*]

[a] Department of Biophysics, Faculty of Science, Palacky University, 17. listopadu 12, CZ-77146 Olomouc, Czech Republic
[b] Institute of Biophysics, Academy of Sciences of the Czech Republic, Kralovopolska 135, 61265 Brno, Czech Republic
[c] Faculty of Pharmaceutical Sciences, Suzuka University of Medical Science, Suzuka 513-8670, Japan

ARTICLE INFO

ABSTRACT

Background: The design of anticancer metallodrugs is currently focused on platinum complexes which form on DNA major adducts that cannot readily be removed by DNA repair systems. Hence, antitumor azolato-bridged dinuclear Pt^{II} complexes, such as [{cis-Pt(NH$_3$)$_2$}$_2$(μ-OH)(μ-pyrazolate)]$^{2+}$ (AMPZ), have been designed and synthesized. These complexes exhibit markedly higher toxic effects in tumor cell lines than mononuclear conventional cisplatin.
Methods: Biophysical and biochemical aspects of the alterations induced in short DNA duplexes uniquely and site-specifically modified by the major DNA adduct of AMPZ, namely 1,2-GG intrastrand cross-links, were examined. Attention was also paid to conformational distortions induced in DNA by the adducts of AMPZ and cisplatin, associated alterations in the thermodynamic stability of the duplexes, and recognition of these adducts by high-mobility-group (HMG) domain proteins.
Results: Chemical probing of DNA conformation, DNA bending studies and translesion synthesis by DNA polymerase across the platinum adduct revealed that the distortion induced in DNA by the major adduct of AMPZ was significantly less pronounced than that induced by similar cross-links from cisplatin. Concomitantly, the cross-link from AMPZ reduced the thermodynamic stability of the modified duplex considerably less. In addition, HMGB1 protein recognizes major DNA adducts of AMPZ markedly less than those of cisplatin.
General significance: The experimental evidence demonstrates why the major DNA adducts of the new anticancer azolato-bridged dinuclear Pt^{II} complexes are poor substrates for DNA repair observed in a previously published report. The relative resistance to DNA repair explains why these platinum complexes show major pharmacological advantages over cisplatin in tumor cells.

© 2012 Elsevier B.V. All rights reserved.

1. Introduction

Di- and trinuclear platinum complexes have attracted much interest as alternative drugs to cisplatin [*cis*-diamminedichloridoplatinum(II)] and its analogs in cancer chemotherapy [1–3]. Azolato-bridged dinuclear Pt^{II} complexes constitute a group of anticancer metallodrugs which exhibit a very promising in vitro cytotoxicity [4,5]. These bifunctional complexes appear to be novel anticancer agents with a mechanism of action different from those of mononuclear cisplatin and its analogs used in the clinic. There is a large body of evidence indicating that the cytotoxicity of platinum complexes correlates with their ability to bind DNA [6–8]. Azolato-bridged dinuclear Pt^{II} complexes interact with DNA, and the DNA binding mode of these Pt^{II} complexes is distinctly different from that of cisplatin and other polynuclear Pt^{II} complexes [4,9,10].

A Pt^{II} drug candidate belonging to the class of antitumor azolato-bridged dinuclear Pt^{II} complexes is [{cis-{Pt(NH$_3$)$_2$}$_2$(μ-OH)(μ-pyrazolate)]$^{2+}$ (AMPZ) (Fig. 1). It contains two platinum centers that are each capable of binding DNA monofunctionally after loss of the bridging hydroxide [9]. Global platination of highly polymeric natural DNA with a random nucleotide sequence with AMPZ gives rise to major 1,2-GG intrastrand cross-links (CLs) similar to cisplatin [11]. Unlike cisplatin, AMPZ induces in highly polymeric DNA only small
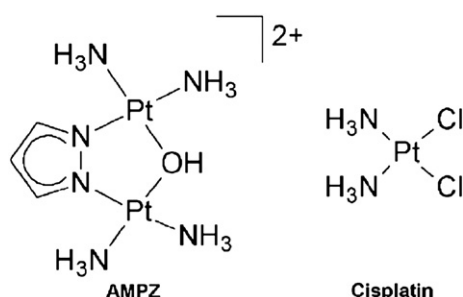
Fig. 1. Structure of cisplatin and azolato-bridged dinuclear Pt^{II} complex.

conformational distortions. In general, after DNA is coordinatively modified by platinum-based anticancer drugs, cellular repair systems recognize this damage and struggle to correct it, which may give rise to the toxic effects of these metallodrugs in tumor cells. This is why DNA repair is considered to play a significant role in modulating the cytotoxicity of platinum drugs [12–14]. The small conformational alterations induced in DNA by AMPZ represent markedly weaker structural motifs recognizable by DNA repair systems compared to distortions induced by cisplatin. This assumption has been experimentally confirmed. We demonstrated in our recent work [11] that DNA adducts of AMPZ can escape repair mechanisms more easily than those of cisplatin, which may potentiate antitumor effects of these new metallodrugs in cancer cells.

The results of previous work [5,11,15] are consistent with the view that major DNA adducts of AMPZ distort the double helical structure of DNA much less than those of conventional cisplatin. Herein, we have studied some important biophysical and biochemical aspects of the alterations induced in short synthetic DNA duplexes uniquely and site-specifically modified by the major DNA adduct of AMPZ, namely 1,2-GG intrastrand CLs. We compare these biophysical and biochemical properties with those obtained under identical conditions for the same adduct of cisplatin. Particular attention is paid to details of conformational distortions induced by the adducts of AMPZ and cisplatin, associated alterations in the thermodynamic stability of the duplexes containing these adducts, and recognition of these adducts by high-mobility-group (HMG) domain protein, that is, the important factors that modulate the antitumor effects of platinum drugs already used in the clinic.

2. Materials and methods

2.1. Chemicals

Cisplatin (purity was ≥99.9% based on elemental and ICP trace analysis) was obtained from Sigma (Prague, Czech Republic). The dinuclear azole-bridged Pt^{II} complex AMPZ was synthesized according to published procedures [4,9]. Stock solutions of the platinum complexes [5×10^{-4} M in NaClO$_4$ (10 mM)] were stored in the dark at 277 K. The concentrations of platinum in the stock solutions were determined by flameless atomic absorption spectrometry (FAAS). Calf thymus (CT) DNA (42% G + C, mean molecular mass ca. 20 000 kDa) was prepared and characterized as described previously [16,17]. T4 DNA ligase, Klenow fragment of DNA polymerase I, and T4 polynucleotide kinase were purchased from New England Biolabs (Beverly, MA). DNA polymerase η (Polη) was from EnzyMax, LLC (Lexington). The synthetic oligodeoxyribonucleotides were purchased from VBC-GENOMICS (Vienna, Austria) or DNA Technology (Aarhus, Denmark). The purity of the oligonucleotides was verified by either high-pressure liquid chromatography (HPLC) or gel electrophoresis. In the present work, the molar concentrations of the single-stranded oligonucleotides or duplexes are related to the oligomers (not to the
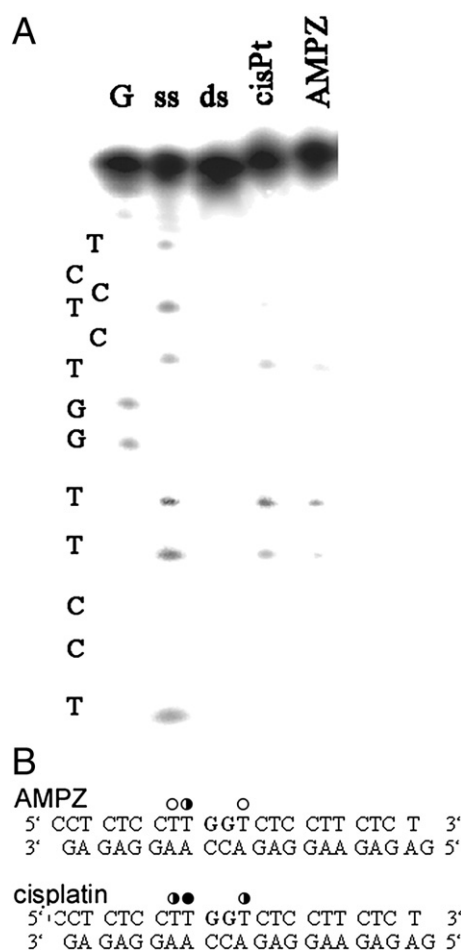

Fig. 2. Chemical probing of DNA conformation. A. Piperidine-induced specific-strand cleavage at KMnO$_4$-modified bases in the 22-bp duplex (shown in Fig. 2B) unplatinated or containing a single, site-specific 1,2-GG intrastrand CL of AMPZ or cisplatin at the central GG residues in the top strand. The oligomers were 5′-end labeled on the top strand. Lanes in Fig. 2A (the top strand 5′-end labeled): G: a Maxam–Gilbert specific reaction for G residues (DMS) in the unplatinated top strand; ss: the unplatinated single strand; ds: the unplatinated duplex; cisPt and AMPZ: the duplex containing a unique adduct of cisplatin and AMPZ, respectively. B. Summary of the reactivity of the chemical probe with the 22-bp duplex containing a single, site-specific adduct of AMPZ and cisplatin. The platinated nucleobase is highlighted in bold. Full, half-full, and open spots designate strong, medium, and weak reactivity, respectively.

monomer content) or double-stranded molecules, respectively. Molar extinction coefficients for the single-stranded oligonucleotides (related to the 12–23-mer strands) were determined by phosphate analysis [18]. The formation of 1:1 complexes between the top strands unmodified or containing the intrastrand adduct and bottom strands of the duplexes was verified by recording isothermal UV absorbance mixing curves at 298 K [19]. The N-terminal His6-tagged xeroderma pigmentosum group A (XPA) protein was obtained by expressing the plasmid DNA pET15b/XPA template [20] in RTS 500 *Escherichia coli* HY (Roche) and purified on Ni^{2+}–NTA agarose and by hydroxyapatite chromatography [21]. The plasmid DNA pET15b/XPA was kindly provided by Richard D. Wood. Acrylamide, bis(acrylamide), NaCN, dithiothreitol, and urea were from Merck KgaA (Darmstadt, Germany). Dimethyl sulfate (DMS) and KMnO$_4$ were from Sigma (Prague, Czech Republic). Deoxyribonucleotide triphosphates (dNTPs) were from Roche Diagnostics, GmbH (Mannheim, Germany). Sodium dodecyl sulfate (SDS) was from Serva (Heidelberg, Germany). Expression and purification of domains A (residues 1–84 [22] and B (residues 85–180 [22]) (HMGB1a and HMGB1b, respectively) of recombinant rat full-length HMGB1 protein (HMG = high mobility group) were carried out as
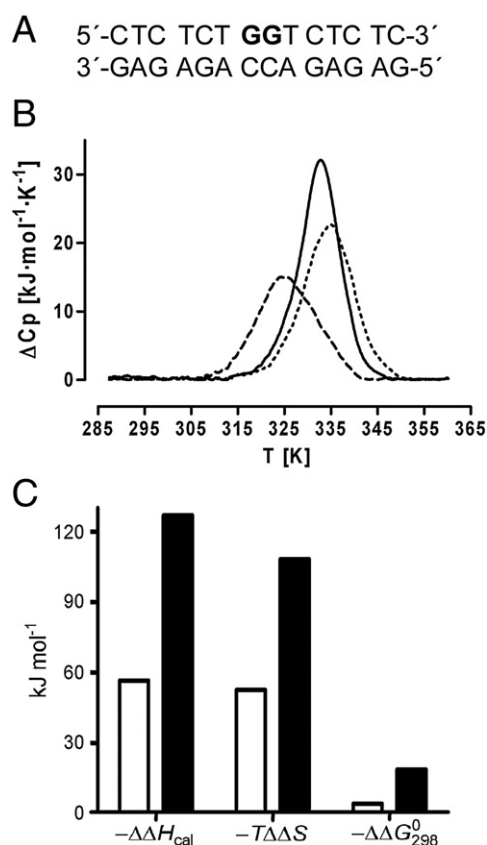
Fig. 3. Differential scanning calorimetry of the unmodified 14-bp duplex and duplexes containing a single, 1,2-GG intrastrand CL of AMPZ or cisplatin. A. Nucleotide sequence of the 14-bp duplex; the bold letters (central G residues) in the top strand indicate the location of the adduct of the Pt^{II} complex. B. DSC thermograms; lines: solid, unmodified duplex; dashed, duplex containing the adduct of cisplatin; dotted, duplex containing the adduct of AMPZ. The duplex concentration was 30 μM, and the buffer conditions were sodium phosphate (NaH_2PO_4/Na_2HPO_4, 10 mM, pH 7.0) and NaCl (150 mM). C. The contributions of enthalpic and entropic effects to the stability (free energy change) of the 14-bp duplex containing the CL of AMPZ (open bars) or cisplatin (solid bars). The units of each parameter ($\Delta\Delta H_{cal}$, $T\Delta\Delta S$, and $\Delta\Delta G^0_{298}$) are kJ mol^{-1} and $T = 298$ K. For other details, see the text.

described [22–24]. Nonidet P-40 was from Fluka (Prague, Czech Republic). Radioactive products were from Amersham (Arlington Heights, IL, USA).

2.2. Platination reactions

CT DNA was incubated with the platinum complex in $NaClO_4$ (10 mM) for 48 h at 310 K in the dark. At the end of the incubation, the samples were exhaustively dialyzed against the medium required for subsequent biochemical or biophysical analysis. An aliquot of these samples was used to determine r_b values (the number of molecules of the platinum complex bound per nucleotide residue) by FAAS. The duplexes containing single, site-specific adducts of the platinum compounds were prepared as follows: the single-stranded oligonucleotides (the top strands of the duplexes used in the present work) were reacted with Pt^{II} complex in the dark. The platinated oligonucleotide was repurified by HPLC. FAAS and optical density measurements were used to verify that the modified oligonucleotides contained one molecule of platinum complex per one strand. By using Maxam–Gilbert (DMS) footprinting of platinum on DNA [25], we also verified that the N7 position of the guanine residue in the platinated top strands was not accessible for reaction with DMS and that these intrastrand adducts were stable in the single- or double-stranded oligonucleotides for at least 7 days. The platinated top strand was

allowed to anneal with the complementary strand in $NaClO_4$ (0.1 M) and incubated at 310 K for 24 h.

2.3. Chemical probing of DNA conformation

The reaction of the platinated oligonucleotide duplexes with $KMnO_4$ was performed as described previously [26]. The top strand of the oligonucleotide duplexes was 5′-end-labeled with [γ-^{32}P]ATP and T4 polynucleotide kinase. In the case of the platinated oligonucleotides, platinum was removed after reaction of the DNA with the probe by incubation with NaCN (0.2 M, pH 11) at 318 K for 16 h in the dark.

2.4. Differential scanning calorimetry (DSC)

Excess heat capacity (ΔC_p) versus temperature profiles for the thermally induced transitions of the 14-bp duplex (see Fig. 3A for its sequence) were measured using a NANO-DSC calorimeter (TA Instruments, Utah, USA). In the DSC experiments the concentration of duplex was 30 μM, the heating rate was 60 K h^{-1}, and the maximum temperature was 368 K. After reaching the maximum temperature the samples were cooled at the same rate to the starting temperature of 283 K. In this study ΔC_p is defined as the excess heat capacity, which is baseline-subtracted and concentration-normalized [27]. The reference scans were subtracted from the sample scans to obtain ΔC_p versus temperature profiles. The enthalpies (ΔH_{cal}) and entropies (ΔS) of duplex melting were calculated from the areas under the experimental ΔC_p versus T and the derived $\Delta C_p/T$ versus T curves, respectively, using ORIGIN (version 5.0, Microcal, Studio City, CA). The free energy of duplex dissociation at 298 K (ΔG^0_{298}) was calculated from the standard thermodynamic relationship and the corresponding ΔH_{cal} and ΔS values:

$$\Delta G^0_{298} = \Delta H_{cal} - 298.15\Delta S. \tag{1}$$

The duplexes were dissolved in buffer, at pH 7.0, containing sodium phosphate (NaH_2PO_4/Na_2HPO_4, 10 mM) and NaCl (150 mM). It was also verified, as described previously [28,29], that the melting transitions of both the platinated and unmodified duplexes were fully reversible.

2.5. DNA synthesis by DNA polymerase η

The 23-mer templates containing a single 1,2-GG intrastrand CL of AMPZ or cisplatin were prepared in the same way as described in the Platination reactions section (*vide supra*). DNA substrates were generated by annealing the 23-mer template containing site-specific adducts of AMPZ or cisplatin to the 12- or 16-mer 5′-^{32}P labeled oligomer primers which were complementary to the 3′ termini of the 23-mer template. In the control undamaged DNA substrates, unplatinated 23-mer template was used. The sequences of DNA substrates containing 23-mer template oligonucleotides annealed to the primers are shown in the corresponding figures.

Polη reactions (50 μL) contained potassium phosphate (pH 7.0, 25 mM), $MgCl_2$ (5 mM), dithiothreitol (5 mM), bovine serum albumin (100 μg mL^{-1}), glycerol (10%), dNTPs (100 μM) and 1 pmol of 5′-^{32}P labeled oligonucleotide primer annealed to an oligonucleotide template. Reactions were initiated by adding Polη (reaction times and enzyme concentrations are indicated in the figures). After incubation for certain time at 303 K, aliquots (10 μL) were withdrawn and the reactions in these aliquots were terminated by the addition of 5 μL of loading buffer containing EDTA (500 mM), bromophenol blue (0.1%) in formamide (90%) and by heating at 363 K for 1 min. The reaction products were resolved on 24% PAA gels containing 8 M urea and then visualized and quantified using a biomolecular imager Typhoon FLA 9500 (GE Healthcare) and AIDA image analyzer software. The extent of translesion synthesis on platinated

Table 1
Calorimetry-derived thermodynamic parameters for the dissociation (melting) of the unmodified and platinum-modified 14-bp duplexes.

Duplex	T_m[a] (K)	ΔH_{cal}[a] (kJ mol^{-1})	ΔS[a] (kJ K^{-1} mol^{-1})	ΔG^0_{298}[a] (kJ mol^{-1})	ΔH_{vH} (kJ mol^{-1})	$\Delta H_{vH}/\Delta H_{cal}$	K_D[b] (µM)
Control	333.0	367.2	1.104	38.0	374.5	1.02	0.2
AMPZ	334.9 (1.9)	310.7 (−56.5)	0.928 (−0.176)	34.0 (−4.0)	313.8	1.01	1.1
Cisplatin	325.5 (−7.5)	240.3 (−126.9)	0.741 (−0.363)	19.4 (−18.6)	247.5	1.03	397.7

[a] The ΔH_{cal} and ΔS values are averages derived from three independent experiments. The experimental uncertainties of the parameters are as follows: $T_m \pm 0.5$ K, $\Delta H_{cal} \pm 2\%$, $\Delta S \pm 3\%$, $\Delta G^0_{298} \pm 3\%$). The "$\Delta\Delta$" parameters are given in parentheses (these parameters are computed by subtracting the appropriate value measured for the control, the unmodified duplex, from the value measured for the duplex containing the single, site-specific platinum adduct.

[b] K_D denotes the dissociation constant for strand dissociation ($\Delta G^0_{298} = -RT\ln K_D$; T is the temperature in Kelvin, and R is the universal gas constant (8.314472 JK^{-1} mol^{-1}).

templates was calculated as the sum of elongation products past the platinum adducts as a percent of total primer termini (elongated and unelongated) according to the following equation:

$$\% \text{ translesion synthesis} = (\text{bypass product}/\text{total primer termini}) \times 100 \qquad (2)$$

where bypass product equals chain elongation past the sites corresponding to the platinum adduct; total primer termini are defined as the sum of elongated and unelongated primers.

2.6. Ligation and electrophoresis of oligonucleotides

Duplexes [16- or 22-base pairs (bp) shown in Fig. 5] unplatinated or containing single, 1,2-GG intrastrand CL of AMPZ or cisplatin were 5′-end-labeled with [γ-^{32}P]ATP by using T4 polynucleotide kinase. The duplexes were allowed to react with T4 DNA ligase. The resulting samples were subsequently examined on 8% native polyacrylamide (PAA) [mono:bis(acrylamide) ratio 29:1] electrophoresis gels. Other details of these experiments were as described in previous papers [30,31] or are described in the text.

2.7. Flow linear dichroism (LD)

Flow LD spectra were collected by using a flow Couette cell in a Jasco J-720 spectropolarimeter adapted for LD measurements. Long molecules, such as DNA (minimum length of ~250 bp), can be orientated in a flow Couette cell. The flow cell consists of a fixed outer cylinder and a rotating solid quartz inner cylinder, separated by a gap of 0.5 mm, giving a total path length of 1 mm. LD spectra of DNA at the concentration of 0.1 mg mL^{-1} modified by the Pt^{II} complexes were recorded at 298 K in NaClO$_4$ (10 mM) plus NaCl (20 mM) and sodium cacodylate (10 mM, pH 7.0) [32,33].

2.8. Electrophoretic mobility shift assays with HMGB1 domain proteins

A radioactively labeled 23-bp DNA probe with blunt ends (its sequence is shown in Fig. 7A) was titrated with HMGB1a or HMGB1b proteins. The duplex (10 nM) was incubated with the proteins in 10 µL sample volumes in a buffer composed of HEPES (10 mM, pH 7.5), MgCl$_2$ (10 mM), LiCl (50 mM), NaCl (0.1 M), spermidine (1 mM), bovine serum albumin (0.2 mg.mL^{-1}), and Nonidet P40 (0.05% v/v). For all gel mobility shift experiments, samples were incubated on ice for 1 h and made 7% in sucrose and 0.017% in xylene cyanol before loading on running, precooled (277 K), prerun (300 V, 1–2 h) 5% native PAA gels [29:1 acrylamide:bisacrylamide, 0.5 × Tris borate–EDTA (TBE) buffer (Tris–HCl (45 mM), boric acid (45 mM), and EDTA (1 mM, pH 8.3)]. Gels were electrophoresed at 277 K and 300 V for ~1.5 h, dried, exposed to a molecular imaging plate, and analyzed on a FUJIFILM bioimaging analyzer. The radioactivities associated with the bands were quantitated with the AIDA image analyzer software. Other details have been published previously [22,34].

2.9. Other physical methods

Absorption spectra were measured with a Beckman 7400 DU spectrophotometer equipped with a thermoelectrically controlled cell holder. HPLC purification of oligonucleotides was carried out on a Waters HPLC system consisting of a Waters 262 pump, Waters 2487 UV detector, and Waters 600S controller with MonoQ 5/50 GL column. The FAAS measurements were carried out on a Varian AA240Z Zeeman atomic absorption spectrometer equipped with a GTA 120 graphite tube atomizer. If not stated otherwise, the gels were visualized on a BAS 2500 FUJIFILM bioimaging analyzer, and the radioactivity associated with bands was quantified with the AIDA image analyzer software (Raytest, Germany).

3. Results

3.1. DNA conformation by a chemical probe

It was demonstrated previously [11] that AMPZ forms preferentially in natural helical DNA with a random sequence 1,2-GG intrastrand CLs similar to cisplatin. To obtain information on how these major adducts affect DNA conformation, oligodeoxyribonucleotide duplexes containing a site-specific 1,2-GG intrastrand CL of AMPZ or cisplatin were further analyzed by a chemical probe of DNA conformation. The platinated 22 bp duplex was treated with the chemical agent, KMnO$_4$, which is used as a probe for structural changes in the vicinity of thymine residues [26,35,36]. This probe reacts preferentially with thymine residues in single-stranded DNA and in distorted double-stranded DNA [26,37]. For this analysis, we used exactly the same methodology as in our recent studies dealing with DNA adducts of various antitumor platinum drugs (for example, see Refs. [26,35,36] for the details of this experiment) Representative gel showing piperidine-induced specific strand cleavage at KMnO$_4$-modified bases in the unplatinated 22 bp duplex or the duplex-containing the single 1,2-GG intrastrand CL of AMPZ or cisplatin are illustrated in Fig. 2A. The results are schematically summarized in Fig. 2B. The pattern and degree of reactivity toward the chemical probe (KMnO$_4$) indicate that the conformational distortion induced by the 1,2-GG intrastrand CL of AMPZ is delocalized, extending over at least five base pairs around the adduct. The distortion induced by the adduct formed by AMPZ appears to be significantly less pronounced than that induced by the CL of cisplatin (Fig. 2). Interestingly, the most pronounced structural perturbations in these adducts are observed at T residues adjacent to the 5′-G contained in the CL.

3.2. Differential scanning calorimetry (DSC)

A calorimetric technique was used to study the effect of the 1,2-GG intrastrand CLs formed by AMPZ on the thermal stability and energetics of a site-specifically platinated 14-bp DNA duplex (Fig. 3A). The thermodynamic stability of the drug-damaged DNA has been shown to play an important role in the cellular response and biological activity of platinum antitumor drugs [28,29,38–42]. Fig. 3B shows DSC melting profiles (ΔC_p versus T) for the parent unmodified 14-bp duplex (solid
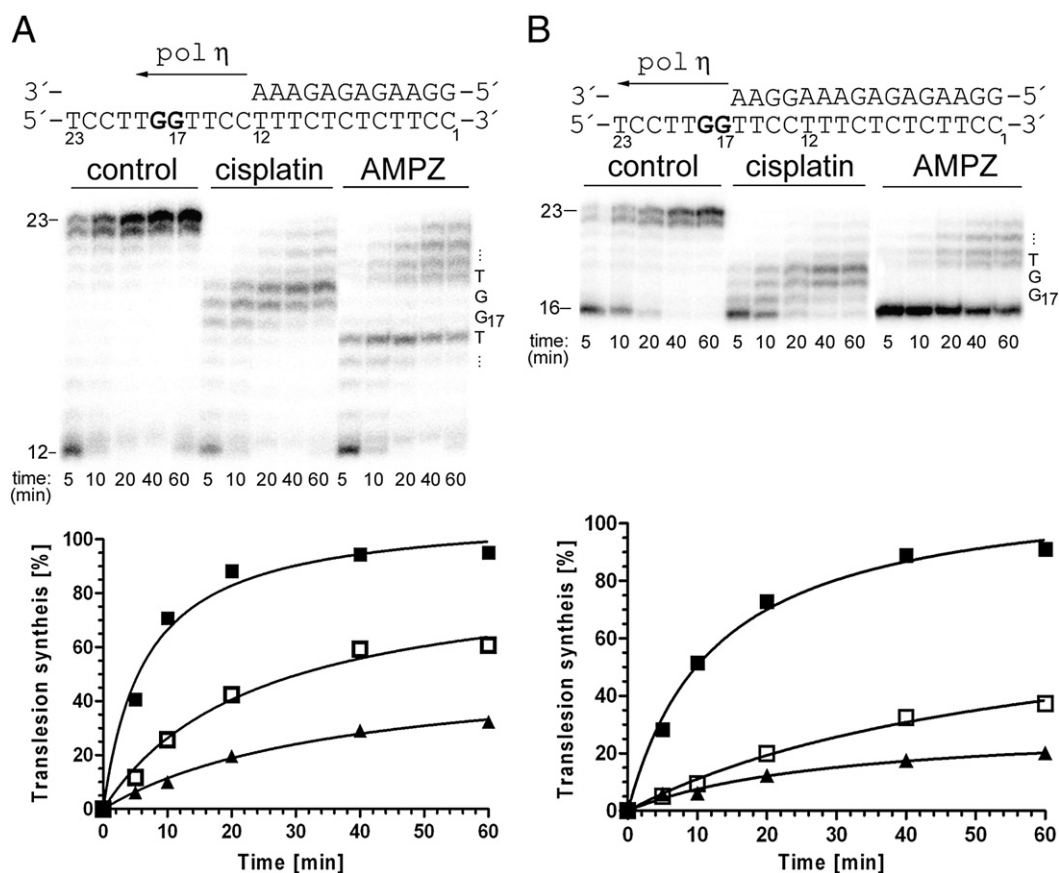
Fig. 4. Primer extension activity of Polη. The experiments were conducted using the 12-mer/23-mer ("running-start" extension) (A) or 16-mer/23-mer ("standing-start" extension) (B) primer-template duplexes (1 pmol) and Polη (80 fmol) in 10 μL for the times indicated. This duplex was unplatinated or contained single, 1,2-GG intrastrand CL formed at the neighboring guanine residues in the TGGT sequence by AMPZ or cisplatin. The nucleotide sequences of the templates and the primers are shown above the representative images of DNA polymerase reaction products resolved on 24% PAA gels in Fig. 4A,B; the bold letters (Gs in the positions 17 and 18 in the TGGT sequence) in the template strand indicate the location of the adduct of the Pt^{II} complex. See the text for details. The strong bands marked 12 and 16 in the autoradiograms shown in Fig. 4A,B correspond to the 12- and 16-mer primers, respectively; the pause site opposite the 3′G in the template is marked G_{17}; the bands marked 23 correspond to the full-length products. The bottom graphs show the time dependences of the inhibition of DNA synthesis on undamaged (control) template (■), DNA containing the adduct of AMPZ (□) or cisplatin (▲). Data are means from three different experiments with two independent template preparations.

curve) and the same duplexes containing a single intrastrand adduct of AMPZ and for comparative purposes also that of cisplatin. Each transition showed negligible changes in the heat capacities between the initial and final states, and denaturation (heating) and renaturation (cooling) curves for the unmodified and platinated duplexes were superimposable (not shown), which is consistent with the reversibility of the melting equilibrium.

Therefore, the calorimetric data were only interpreted for the duplex containing the 1,2-GG intrastrand CL of AMPZ. This interpretation was based on the assumption that the thermodynamic parameters for the melting of the unmodified and platinated duplexes can be ascribed to differences in the initial duplex states. This implies that the final single-stranded states should be thermodynamically equivalent at the elevated temperatures at which they are formed. This assumption was verified (not shown) similarly to earlier reports by recording identical circular dichroic spectra for samples of unplatinated and platinated duplexes heated at high temperatures (363 K) [28,29,39,40].

DSC melting profiles (Fig. 3B) were analyzed as described in the section Materials and methods and the results are listed in Table 1. All thermodynamic parameters discussed in this work refer to the duplex dissociation process. Differences in the thermodynamics of strand dissociation due to the presence of a platinum adduct are presented as "ΔΔ" parameters. These parameters are computed by subtracting the appropriate value measured for the control, the unmodified duplex,

from the value measured for the duplex containing the single, site-specific platinum adduct and are reported in Table 1 in parentheses.

Inspection of these thermodynamic parameters reveals a number of interesting features. First, the formation of the 1,2-GG intrastrand CL of AMPZ increased the duplex thermal stability by 1.9 K, whereas the formation of the same adduct of cisplatin decreased the duplex thermal stability by 7.5 K. However, changes in melting temperature (T_m) are not necessarily good predictors of changes in thermodynamic stability (free energy of duplex melting, ΔG^0) because there is no simple correspondence between changes in T_m and ΔG^0 due to the presence of a lesion in DNA [43,44]. The reason for the failure of changes of T_m values to reflect reliably the lesion-induced changes in thermodynamic stability (changes of ΔG^0 values) is neglect of the temperature dependence of the duplex stability. T_m values reflect the behavior of the duplex at high temperature whereas the free-energy changes are evaluated for a low temperature standard state, typically 298 K; these low-temperature standard states correspond to the temperature domain of the processes of biological significance. Therefore, in the present work, we compared the effects of the lesions induced by single, site-specific 1,2-GG intrastrand CLs of AMPZ or cisplatin and contained in short oligodeoxyribonucleotide duplexes on DNA stability with emphasis on the thermodynamic origins of that stability.

Interestingly, the formation of the CL by AMPZ resulted in a decrease in the enthalpy of duplex dissociation (Table 1, Fig. 3C). In
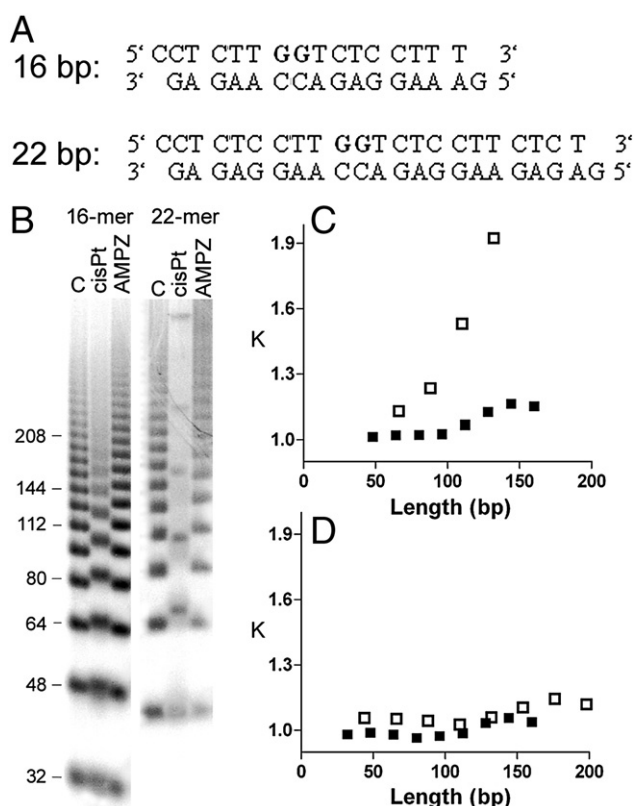
Fig. 5. Ligation and electrophoresis of oligodeoxyribonucleotide duplexes containing single, site-specific 1,2-GG intrastrand CL of AMPZ or cisplatin. A. Sequences of the synthetic oligodeoxyribonucleotides used in this study. The top and bottom strands of each pair are designated 'top' and 'bottom', respectively, in the text. The bold letters in the top strand indicate the location of the adduct after the modification of the oligonucleotides by AMPZ or cisplatin as described in the text. B. Autoradiogram of the ligation products of oligonucleotide duplexes 16 bp and 22 bp long; platinum-free duplexes (lanes C) and duplexes containing a unique adduct of cisplatin or AMPZ separated on an 8% polyacrylamide gel (lanes cisPt and AMPZ, respectively). C and D. Plots showing the relative mobility K (defined as the ratios of the calculated and the actual lengths) versus actual sequence length for the 16- (■) and 22-bp (□) oligomers containing the adduct of cisplatin (C) and AMPZ (D). The experimental points represent the average of three independent electrophoresis experiments.

other words, the 1,2-GG intrastrand CL of this platinum complex enthalpically destabilized the duplex relative to its unmodified counterpart. On the other hand, the formation of the CL by AMPZ also resulted in a decrease in the duplex dissociation entropy (Table 1, Fig. 3C). Thus, the net result of these enthalpic and entropic effects was that the formation of the 1,2-GG intrastrand CL by AMPZ induced only a very small decrease (4.0 kJ mol^{-1}) in the free energy of duplex dissociation at 298 K (ΔG^0_{298}) (Table 1, Fig. 3C). In contrast, the formation of the CL by cisplatin resulted in a considerably larger decrease in the enthalpy and entropy of duplex dissociation (Table 1, Fig. 3C) in accord with the previously reported observations [28,39]. The net result of these enthalpic and entropic effects was that the formation of the 1,2-GG intrastrand CL by cisplatin induced a much larger (~5-fold) decrease (18.6 kJ mol^{-1}) in the free energy of duplex dissociation at 298 K (ΔG^0_{298}) (Table 1, Fig. 3C).

Further analysis of the nature of a thermal transition of DNA duplexes intrastrand cross-linked by AMPZ provides a quantitative comparison of the model-independent calorimetric (ΔH_{cal}) and model-dependent van't Hoff (ΔH_{vH}) transition enthalpy. The $\Delta H_{vH}/\Delta H_{cal}$ ratio makes it possible to decide whether the transition proceeds in a two-state (all-or-none) manner or whether the transition includes intermediate states that are responsible for broadening the thermograms [45]. The ΔH_{vH} enthalpy values can be obtained by analyzing the shape of each calorimetric curve using the approach reported earlier [45]. If the $\Delta H_{vH}/\Delta H_{cal}$ ratio is equal to 1, then the transition takes
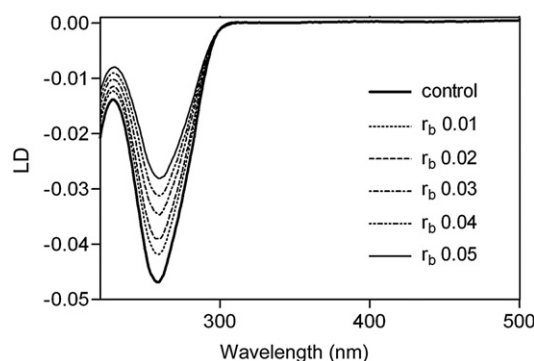

Fig. 6. Linear dichroism (LD) spectra of CT DNA modified by AMPZ. LD spectra were recorded for DNA in NaClO$_4$ (10 mM) with NaCl (20 mM) and sodium cacodylate (10 mM, pH 7.0) at 298 K. The concentration of DNA was 100 μg mL^{-1}.

place in an all or-nothing fashion. As shown in Table 1, we obtained ratios in the range of 1.01–1.03 for the duplex and platinum compounds tested in this work, thus confirming the two-state melting behavior.

Based on the calorimetric data, the energetic consequences of the 1,2-GG intrastrand CL of AMPZ and cisplatin are strikingly different. While the major CL of cisplatin significantly reduces the thermodynamic stability of the modified duplex, the CL of AMPZ affects the thermodynamic stability of the modified duplex negligibly (Table 1, Fig. 3C).

3.3. Inhibition of DNA polymerization

It has been demonstrated that DNA modifications by various transition metal-based complexes have significant effects on processing by a number of prokaryotic, eukaryotic, and viral DNA polymerases [46–52]. Interestingly, with DNA templates containing site-specifically placed adducts of various platinum compounds, a number of DNA polymerases are blocked but others can also traverse through platinum adducts, depending on their character and conformational alterations induced in DNA.

Polη is DNA polymerase capable of translesion synthesis past a number of bulky DNA adducts including those of platinum antitumor drugs. We investigated in the present work the ability of Polη to catalyze translesion synthesis past major 1,2-GG intrastrand CLs of AMPZ or cisplatin in vitro. We used templates site-specifically modified by the 1,2-GG intrastrand CL of AMPZ or cisplatin. These adducts differ in the capability to distort DNA (*vide supra*), which inversely correlates with the toxic efficacy of the drugs in several tumor cell lines [4]. This study was designed to answer the following question: can Polη, when it processes DNA substrates containing 1,2-GG intrastrand CLs of AMPZ or cisplatin, reveal differences in alterations imposed on DNA by these adducts?

The distinction was made in the past between standing-start (or initiation mode) bypass and running-start (elongation mode) bypass. In the former, the primer terminus is located opposite the nucleotide preceding the lesion, and thus, synthesis begins with insertion opposite the lesion. In the latter mode, the primer terminus is located upstream of the lesion, and thus, replication is initiated at an unperturbed primer-template configuration; the polymerase encounters the lesion during the elongation mode of polymerization. We constructed the 12-mer/23-mer or 16-mer/23-mer primer-template duplexes (see the upper parts of Fig. 4A and B) unplatinated or containing a single 1,2-GG intrastrand CL of AMPZ or cisplatin. The first 12 or 16 nucleotides on the 3′ terminus of the 23-mer template strand were complementary to the nucleotides of the 12-mer or 16-mer primers, respectively so that the 3′ guanine residues involved in the adduct on the template
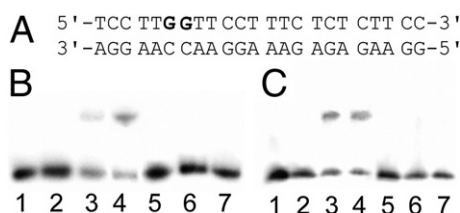
A 5'-TCC TT**GG**TT CCT TTC TCT CTT CC-3'
   3'-AGG AAC CAA GGA AAG AGA GAA GG-5'

Fig. 7. Gel mobility shift assay analysis of the interaction of a 23 bp duplex containing the 1,2-GG intrastrand CL of cisplatin or AMPZ with HMGB1a and HMGB1b. Radioactively labeled oligodeoxyribonucleotide duplexes (10 nM) were incubated with HMGB1a or HMGB1b. A. Sequence of the synthetic oligodeoxyribonucleotide duplex used in this study. B, C. Autoradiograms of the gel mobility shift assay analysis of the interaction with HMGB1a (B) and HMGB1b (C); the reaction volume was 10 μL. Lanes: 1 — control (unplatinated) duplex; 2–4 — duplex containing 1,2-GG intrastrand CL of cisplatin; 5–7 — duplex containing 1,2-GG intrastrand CL of AMPZ. Lanes 2, 5 — no protein added; Lanes 3, 6 — 5 ng of HMGB1a (B) or 20 ng of HMGB1b added (C); Lanes 1, 4, 7 — 10 ng of HMGB1a (B) or 40 ng of HMGB1b added (C).

strand were located at its 17th position from the 3′ terminus (Fig. 4A). After annealing the 12- or 16-nucleotide primer to the 3′ terminus of the unplatinated or platinated template strand [positioning the 3′-end of the primer four bases prior to the adduct or immediately prior to the adduct in the template strand (running or standing start extension, respectively)], we examined elongation of primers on undamaged DNA templates along with DNA polymerization through the adduct of AMPZ or cisplatin by Polη in the presence of all four dNTPs. In these experiments primer/templates were used in an approximately 12.5-fold excess over enzyme. The reaction was stopped at various time intervals, and the products were analyzed using a sequencing gel (see autoradiograms in Fig. 4).

When untreated primer-template was used, major bands corresponding to the full-length (23 nt) product and the product one nucleotide shorter (22 nt) were observed (see autoradiograms in Fig. 4, lanes control). The products corresponding to these bands accumulated with time.

Primer extension on damaged templates produced multiple shorter elongation products, and no full-length products (23 nt and 22 nt) were seen (see autoradiograms in Fig. 4, lanes cisplatin and AMPZ). Relative distribution of the products of replication depended on the structure of platinum adduct and reaction time. Autoradiograms in Fig. 4 (lanes cisplatin and AMPZ) show primer extension on templates containing a cisplatin- or AMPZ-GG adduct and bottom graphs in Fig. 4 summarize translesion synthesis past both Pt-DNA diadducts. The distribution of the products of primer elongation on the template containing 1,2-GG intrastrand CL of AMPZ by Polη was different from that seen with the template containing the same CL of cisplatin. Primer extension on template containing 1,2-GG intrastrand CL of cisplatin was inhibited at three major sites: the sites opposite both the 3′- and 5′Gs of the platinum adduct and the site immediately following the platinum adduct. The pause sites opposite the 3′- and 5′Gs are thought to represent inhibition of nucleotide incorporation opposite the 5′G of the platinum adduct and inhibition of elongation from the 5′G, respectively. Similarly, the pause site immediately following the platinum adduct is thought to represent inhibition of elongation from the T adjacent to 5′G of the adduct. The stop site across the 3′ cisplatinated G became less prominent with increasing incubation time, while intensities of the bands corresponding to the stop sites across the sites following the platinum adduct increased.

In contrast, primer extension by Polη on templates damaged by the CL of AMPZ produced only one strong pause site just prior to the adduct which is thought to indicate an inhibition of nucleotide incorporation opposite the 3′G of the platinum adduct. Interestingly, no pause sites opposite both the 3′- and 5′Gs of the platinum adduct were seen, and

the stop sites across the sites following the platinum adduct were clearly visible. Also importantly, the stop-site across the pause site just prior to the adduct became less prominent with increasing incubation time, while intensities of the bands corresponding to the stop sites across the sites following the platinum adduct increased.

The extent of Polη-catalyzed translesion synthesis past the AMPZ-GG and cisplatin-GG adducts (calculated by Eq. (2); see Materials and methods) is shown in graphs on the bottom of Fig. 4. Translesion synthesis relative to synthesis on an undamaged template (calculated by Eq. (2)) was significantly higher for AMPZ adducts than for cisplatin adducts. These data support our thesis that the translesion synthesis past Pt-DNA adducts may be determined at least in part by distinct structural characteristics of DNA 1,2-GG intrastrand CLs of AMPZ and cisplatin. Fig. 4 also indicates that there was no qualitative difference in the bypass when running start and standing start extensions were compared.

3.4. A phase-sensitive gel electrophoresis bending assay

The top strands of the oligonucleotide duplexes were designed to contain only one high-affinity platinum binding site, the two adjacent guanine bases of the intrastrand CL (Fig. 5A). The sequences were designed to leave a 1 bp overhang at its 5′-ends in double-stranded form. These overhangs facilitate polymerization of the monomeric oligonucleotide duplexes by T4 DNA ligase in only one orientation, and maintain a constant interadduct distance throughout the resulting multimer. An autoradiogram of electrophoresis gel revealing resolution of the ligation products of 16- and 22 bp duplexes (Fig. 5A) containing a unique 1,2-GG intrastrand CL of AMPZ or cisplatin is shown in Fig. 5B. Major DNA adducts of cisplatin or azolato-bridged dinuclear Pt^{II} complexes locally unwind DNA by 15–20° [5,53]. Thus, the 22-bp sequence repeat yields 22-bp phasing of platinum adducts corresponding approximately to two helical repeats, allowing eventual bends to add constructively. In contrast, 16-bp phasing of the adducts corresponds approximately to one-and-a-half-helical repeat, i.e. the adducts are almost perfectly dephased and any directed bends will add destructively, preventing any appreciable anomalous mobility shifts.

In accord with the previously published data [53–55], a significant retardation was observed for the multimers of 22-bp duplexes containing single, 1,2-GG intrastrand CL of cisplatin and a relatively very small retardation was observed for the multimers of cisplatinated 16-bp duplexes. In contrast, almost negligible retardation was observed for the multimers of both 16-bp and 22-bp duplexes modified by the 1,2-intrastrand CL of AMPZ. The K factor (relative mobility) is defined as the ratio of calculated length of a multimer its real length. The higher this ratio, the more bent is a given oligomer. A K value of 1 means that the oligomer migrates as though it had no bends [30]. The calculated length is based on a multimer's mobility, and is obtained from a calibration curve constructed from the mobilities of unplatinated multimers labeled C in Fig. 5. The variations of the K factor versus sequence length obtained for the multimers of the duplexes 16 and 22 bp long and containing the unique 1,2-GG intrastrand CL of cisplatin and AMPZ are shown in Fig. 5C and D, respectively. The K value obtained for the multimers of the duplex 22 bp long and containing the intrastrand CL of cisplatin increases dramatically with DNA length, resembling the electrophoretic behavior of bent DNA molecules in which the sequence repeat closely matches the double helix screw repeat [56]. Furthermore, the mobility was relatively unaltered in cisplatinated duplex DNA molecules containing platinum atoms repeated at 16-bp intervals, representing a phasing of ~1.5 helical turns. This latter control assures that the gel mobility changes are not simply due to charge or localized frictional effects of the $[Pt(NH_3)_2]^{2+}$ adduct. In contrast, the plots obtained for the multimers of the duplexes 16 and 22 bp long and containing the intrastrand CL of AMPZ appear as an almost horizontal line passing through the value $K = 1$ indicating no curvature [30].

3.5. Linear dichroism

Binding of AMPZ to CT DNA was also monitored by LD spectroscopy (Fig. 6). It is well established that the magnitude of the LD signal measured within the DNA absorption band (e.g., at the 258 nm maximum) is a function of its persistence length. It is known that the formation of rigid bends, kinks or changes in flexibility induced by strongly bound compounds, can manifest themselves as decreases in the abilities of the modified DNA molecules to align themselves in the hydrodynamic flow gradient of the LD cell. The magnitudes of the LD signals at 258 nm decrease as a function of r_b for AMPZ (Fig. 6).

3.6. Recognition of adducts by HMG domain proteins

An important feature of the mechanism of action of cisplatin is that the altered structures produced by the bending of the helical axis induced in DNA by 1,2-intrastrand CLs of cisplatin attract HMG domain proteins and other proteins [7,57,58]. This binding of HMG domain proteins to cisplatin-modified DNA has been postulated to mediate or enhance the drug's antitumor properties [57]. Full-length HMGB1 or HMGB2 proteins and the domains A and B of HMGB1 protein (HMGB1a and HMGB1b, respectively) bind to 1,2-GG intrastrand CLs of cisplatin.

Since the DNA conformational changes caused by 1,2-intrastrand CLs of AMPZ are very different from those caused by cisplatin, experiments were performed to determine if differences exist in the recognition of the 1,2-intrastrand CLs of AMPZ and cisplatin by HMG domain proteins. The interactions of the domains A and B of HMGB1, which is considered the prototype of this family of proteins, with the adducts of AMPZ and cisplatin were investigated using a gel mobility shift assay [22,59]. In these experiments, the 23-bp duplex with blunt ends (see Fig. 7A for its sequence) was modified so that it contained a single, site-specific, 1,2-intrastrand CL formed by AMPZ or for comparative purposes by cisplatin. The binding of the domains HMGB1a or HMGB1b to these DNA probes was detected as a band of reduced electrophoretic mobility on the gels [22,59]. These proteins exhibited negligible binding to the unmodified 23-bp duplexes, whereas both HMGB1a and HMGB1b recognized and bound to the duplex containing the 1,2-GG intrastrand CL of cisplatin. The results of the incubation of the duplexes modified with AMPZ with HMGB1a or HMGB1b indicate that neither of these proteins bound the probes under conditions where the HMGB1a or HMGB1b proteins associated with the duplex containing the 1,2-GG intrastrand CL of cisplatin (Fig. 7B,C). Hence, the major 1,2-GG intrastrand CLs of AMPZ are either not recognized at all by HMG domain proteins, or the affinity of these proteins is markedly lower for the adducts of AMPZ than for the 1,2-GG intrastrand CL of cisplatin.

4. Discussion

We have demonstrated in our recent work that the DNA binding mode of AMPZ, which exhibits markedly higher toxic effects in some tumor cell lines than conventional mononuclear cisplatin, forms in natural DNA major 1,2-GG intrastrand CLs similar to cisplatin, but in contrast to cisplatin it induces in DNA only small conformational distortions [11]. The pharmacological activity of several metallodrugs is modulated by the "downstream" effects of damaged DNA, such as recognition of damaged DNA by specific proteins and/or repair of this damage [14,58]. In addition, distortion of DNA conformation induced by metallodrugs and changes in the thermodynamic stability of DNA induced by the damage represent important factors that affect these "downstream" cellular events [39,44,60,61]. Thus, to assess how these factors might assert themselves in the cellular processing of DNA damage induced by AMPZ, we characterized further major DNA adducts of this azolato-bridged dinuclear Pt[II] complex by using a chemical probe of DNA conformation, phase-

sensitive gel electrophoresis bending assay and DSC. An analysis of conformational distortions induced in DNA by major CLs of AMPZ and cisplatin revealed substantial differences in the character of these distortions. Their analysis by the chemical probe of DNA conformation demonstrated (Fig. 2) that the distortion induced by the CLs extended over at least 5 bp, although distortion induced by AMPZ was weaker than that induced by cisplatin. Nevertheless, these data suggest that the adducts of both AMPZ and cisplatin should thermodynamically destabilize DNA and that the DNA should be destabilized significantly more by the CL of cisplatin than by that of AMPZ. The results of the DSC analysis (Table 1) are consistent with these suggestions.

DSC can provide quantitative, model-independent characterization of the effects of the lesion on duplex thermodynamics. The duplex melting temperature (thermal stability parameter, T_m), and thermodynamic stability parameters of the duplex dissociation enthalpies (ΔH_{cal}) and entropies (ΔS), derived from analyses of the calorimetrically measured excess heat capacity (ΔC_p), versus temperature profiles are listed in Table 1 along with the corresponding ΔG^0_{298} values calculated at 298 K. Analysis of the T_m values reveals that the adduct of AMPZ even slightly enhances the thermal stability of DNA (by 1.9 K), whereas the same adduct of cisplatin markedly reduces thermal stability of DNA. However, the melting temperature is not a thermodynamic parameter. Therefore, we also examined how the introduction of the 1,2-GG intrastrand CL of AMPZ and cisplatin affects the thermodynamic stability (ΔG^0_{298}) of the DNA duplex. The thermodynamic parameters derived from DSC data reveal that the adduct of cisplatin destabilizes the double helix tested in this work markedly more than the CL of AMPZ, as indicated by an 18.6 kJ mol^{-1} versus only 4.0 kJ mol^{-1} decrease in the Gibbs free energy for dissociation of duplex containing the CL of cisplatin and AMPZ, respectively at 298 K (Table 1). Interestingly, these $\Delta\Delta G^0_{298}$ values represent an equilibrium preference for the unmodified duplexes over those modified by cisplatin or AMPZ of, respectively, 1988 or 5.5 to 1. Thus, these results are consistent with the thesis that the major adduct of AMPZ decreases thermodynamic stability of DNA only negligibly in contrast to the same adduct of cisplatin which enhances the thermodynamic destabilization of DNA markedly. This marked difference in the efficiency of the CLs of cisplatin and AMPZ to thermodynamically destabilize DNA is apparently associated with a markedly different capability of these adducts to distort the DNA conformation.

Inspection of Table 1 also shows that the melting of each duplex accompanied by unfavorable free-energy terms results from characteristic compensation of unfavorable enthalpy and favorable entropy terms. In general, the unfavorable enthalpy terms correspond mainly to the disruption of the base-pair stacks, whereas the favorable entropy terms arise from contributions of the favorable dissociation of two strands and the release of counterions and water molecules. In short, relative to the unmodified parent duplex, their transition enthalpies can be perturbed by as much as 127 or 57 kJ mol^{-1}, respectively, by the CL of cisplatin or AMPZ.

The magnitude of this effect of the 1,2-GG intrastrand CL of cisplatin represents a loss of ~35% of the total enthalpy of dissociation of the parent duplex although only 2 of the 14 base pairs are chemically altered. On the basis of nearest-neighbor predictions [62], complete loss of stacking on both sides of the platinated d(GG) sequence of the 14-bp duplex used in this study is expected to reduce the value of ΔH_{cal} considerably less. In contrast, the magnitude of this effect of adducts of AMPZ represents a loss of only ~15% of the total enthalpy of dissociation of the parent duplex. The observed endothermic enthalpies result primarily from the endothermic heats for the disruption of base pairs and base–base stacks in the duplex. Hence, the formation of the 1,2-GG intrastrand CL by cisplatin is more deleterious energetically than the complete loss of stacking on both sides of the unmodified GG/CC base pairs at that site. Moreover, the transition enthalpy of duplex containing the same CL of AMPZ is perturbed by

the adduct formation by only ~57 kJ mol^{-1}. These observations can be explained in terms of a considerably more extensive decrease in stacking interactions caused by the CL of cisplatin compared with the same adduct of AMPZ, which results from different conformational alterations induced by these adducts.

The changes in the thermodynamic stability of the duplex examined in this work, $\Delta\Delta G^0_{298}$, caused by the formation of a single site-specific 1,2-GG intrastrand CL of cisplatin and AMPZ reflect a combination of enthalpic ($\Delta\Delta H_{cal}$) and entropic ($\Delta\Delta S$) effects. The relative contributions of the CL-induced changes in the enthalpy and entropy terms for the disturbance of the 14-bp duplex can be seen in Fig. 3C. Interestingly, the differences in the transition free-energy change ($\Delta\Delta G^0_{298}$) observed upon formation of the 1,2-GG intrastrand CLs of cisplatin and AMPZ are significantly smaller than the observed differences in the transition enthalpy change ($\Delta\Delta H_{cal}$) (Fig. 3C). The values of $\Delta\Delta H_{cal}$ range from -57 to -127 kJ mol^{-1}, whereas the values of $\Delta\Delta G^0_{298}$ range from only -4 to -19 kJ mol^{-1}. Regardless of the magnitude of $\Delta\Delta H_{cal}$, there is a considerable, but not complete, compensating change in the entropy term. Interestingly, the higher transition enthalpy change due to the CLs is accompanied by a higher entropic compensation. The impact of the 1,2-GG intrastrand CLs of cisplatin and AMPZ on the enthalpy is always destabilizing, whereas the entropy term is always stabilizing. The compensation does not result in invariant stability with respect to the type of Pt^{II} complex.

The $\Delta H_{vH}/\Delta H_{cal}$ ratio makes it possible to determine whether duplex-unfolding takes place in two-state transitions or through the formation of intermediates [45]. If the $\Delta H_{vH}/\Delta H_{cal}$ ratio is equal to 1 then the transition takes place in an all-or-none fashion [45]. We obtained $\Delta H_{vH}/\Delta H_{cal}$ ratios in the range of 1.01–1.03 (Table 1), which confirms that each duplex examined in this work unfolds in a two-state transition. Hence, despite affecting the thermal and thermodynamic parameters of the unfolding of the host duplexes, cisplatin and AMPZ do not affect the properties of DNA to the extent that they would markedly change the cooperativity of the melting transition of the host duplex.

Interestingly, translesion DNA polymerase Polη (which is not a replicative or repair DNA polymerase) when it processes DNA substrates containing 1,2-GG intrastrand CLs of AMPZ or cisplatin reveals differences in alterations imposed on DNA by these adducts. Our data show (Fig. 4) that Polη catalyzes translesion synthesis past GG adducts of AMPZ with greater efficiency than past the same adducts of cisplatin. This result can be interpreted to mean that the less-distorting conformational change induced in template by AMPZ-GG adduct makes it easier for Polη bypass this adduct in comparison with the bypass of cisplatin-GG adducts. It also implies that the increase in translesion synthesis catalyzed by Polη past AMPZ adducts compared to cisplatin adducts is determined primarily by differences in the conformation of DNA at the site of the AMPZ- or cisplatin-GG adducts rather than differences in their bulkiness. However, the greater bulkiness of the AMPZ adducts may be responsible for the observation that primer extension by Polη on templates damaged by the CL of AMPZ produced the first strong pause site just prior to the adduct, i.e. by one nucleotide before the first strong pause site produced by the CL of cisplatin (Fig. 4A).

Multimers of the 22-bp duplex containing single, site-specific 1,2-GG intrastrand CL of cisplatin show strong anomalies in their electrophoretic mobilities as a consequence of coherent addition of in-phase platinum-induced bends [55]. Decrease of the sequence repeat of the cisplatinated site to 16 bp yields multimers of nearly normal mobility because the bends are out of phase. In contrast, the multimers of the 22-bp duplex containing the 1,2-GG intrastrand CLs of AMPZ (shown in lanes AMPZ of Fig. 5B) exhibit virtually no gel mobility shifts, migrating at almost exactly the same positions as unplatinated ladder of multimers. These results show that DNA modified by 1,2-GG intrastrand CLs of AMPZ is not bent consistent with a ^{1}H NMR study of the 10-bp duplex containing 1,2-GG intrastrand CL of AMPZ [5].

The observation that the major adducts of AMPZ do not bend DNA longitudinal axis may help to interpret changes in LD spectra of DNA modified by AMPZ. It is known that the formation of rigid bends or kinks induced by strongly bound compounds, can manifest themselves as decreases in the abilities of the modified DNA molecules to align themselves in the hydrodynamic flow gradient of the LD cell [63]. Thus, it may seem surprising that the magnitudes of the LD signals at 258 nm decrease as a function of r_b for AMPZ (Fig. 6). It is also known that increase of flexibility of DNA may result in a decrease of the LD signal at 258 nm as well. It is, therefore, reasonable to suggest that the formation of strongly bound adducts derived from AMPZ is accompanied by the appearance of flexible hinge joints at the site of the lesion.

An important consequence of the small extent of bending in DNA modified with AMPZ is the lack of recognition of the damage by HMG domain proteins (Fig. 7). HMG domain proteins have been implicated in the cytotoxicity of cisplatin in several types of tumor cells [57,58]. The role of HMG domain proteins as mediators or enhancers of cisplatin-triggered cytotoxicity is because HMG protein binding protects the 1,2-intrastrand CLs of cisplatin from cellular repair [57,58]. This suggests that binding of proteins that have a high affinity for the rigidly bent DNA does not play a role in the mechanism of action of AMPZ.

Recent clinical studies suggest that high levels of expression of proteins associated with removal of adducts of cisplatin from DNA result in tumor resistance and, ultimately, are responsible for the low efficacy of classical platinum-based regimens [64,65]. DNA repair systems most efficiently recognize and remove irreversible DNA adducts that are bulky in nature or severely distort and thermodynamically destabilize double-stranded DNA [14,39,42,61,66,67]. Adducts that cause local unstacking of nucleobases, disruption of Watson-Crick hydrogen bonding, or bending of the DNA helix are ideal substrates for the DNA repair complexes [21]. Thus, based on the outcome of our experiments in cell-free systems, the 1,2-intrastrand CLs produced by AMPZ should be poor substrates for DNA repair. The relative resistance to DNA repair would explain why AMPZ shows major pharmacological advantages over cisplatin in several tumor cells [4].

Acknowledgements

References

[1] J.B. Mangrum, N.P. Farrell, Excursions in polynuclear platinum DNA binding, Chem. Commun. 46 (2010) 6640–6650.

[2] N. Farrell, Polynuclear platinum drugs, in: A. Sigel, H. Sigel (Eds.), Metal Ions in Biological Systems, vol. 42, Marcel Dekker, Inc., New York, Basel, 2004, pp. 251–296.

[3] K.S. Lovejoy, S.J. Lippard, Non-traditional platinum compounds for improved accumulation, oral bioavailability, and tumor targeting, Dalton Trans. (2009) 10651–10659.

[4] S. Komeda, M. Lutz, A. Spek, M. Chikuma, J. Reedijk, New antitumor-active azole-bridged dinuclear platinum(II) complexes: synthesis, characterization, crystal structures, and cytotoxic studies, Inorg. Chem. 39 (2000) 4230–4236.

[5] S. Teletchéa, S. Komeda, J.-M. Teuben, M.A. Elizondo-Riojas, J. Reedijk, J. Kozelka, A pyrazolato-bridged dinuclear platinum(II) complex induces only minor distortions upon DNA-binding, Chem. Eur. J. 12 (2006) 3741–3753.

[6] E.R. Jamieson, S.J. Lippard, Structure, recognition, and processing of cisplatin–DNA adducts, Chem. Rev. 99 (1999) 2467–2498.

[7] V. Brabec, DNA modifications by antitumor platinum and ruthenium compounds: their recognition and repair, Prog. Nucleic Acid Res. Mol. Biol. 71 (2002) 1–68.

[8] V. Brabec, J. Kasparkova, Modifications of DNA by platinum complexes: relation to resistance of tumors to platinum antitumor drugs, Drug Resist. Updat. 8 (2005) 131–146.

[9] S. Komeda, H. Ohishi, H. Yamane, M. Harikawa, K. Sakaguchi, M. Chikuma, An NMR study and crystal structure of [{cis-Pt(NH$_3$)$_2$(9EtG-κN7)}$_2$-(μ-pz)][NO$_3$]$_3$(9EtG) 9-ethylguanine) as a model compound for the 1,2-intrastrand GG cross-link, J. Chem. Soc. Dalton Trans. (1999) 2959–2962.

[10] S. Komeda, M. Lutz, A.L. Spek, Y. Yamanaka, T. Sato, M. Chikuma, J. Reedijk, A novel isomerization on interaction of antitumor-active azole-bridged dinuclear platinum(II) complexes with 9-ethylguanine. Platinum(II) atom migration from N2 to N3 on 1,2,3-triazole, J. Am. Chem. Soc. 124 (2002) 4738–4746.

[11] J. Mlcouskova, J. Kasparkova, T. Suchankova, S. Komeda, V. Brabec, DNA conformation and repair of polymeric natural DNA damaged by antitumor azolato-bridged dinuclear Pt^{II} complex, J. Inorg. Chem. 114 (2012) 15–23.

[12] D. Wang, S.J. Lippard, Cellular processing of platinum anticancer drugs, Nat. Rev. Drug Discov. 4 (2005) 307–320.

[13] L. Kelland, The resurgence of platinum-based cancer chemotherapy, Nat. Rev. Cancer 7 (2007) 573–584.

[14] V. Brabec, J. Kasparkova, Role of DNA repair in antitumor effects of platinum drugs, in: N. Hadjiliadis, E. Sletten (Eds.), Metal Complex–DNA Interactions, Wiley, Chichester, UK, 2009, pp. 175–208.

[15] S. Komeda, S. Bombard, S. Perrier, J. Reedijk, J.F. Kozelka, Kinetic study of azole-bridged dinuclear platinum(II) complexes reacting with a hairpin-stabilized double-stranded oligonucleotide, J. Inorg. Biochem. 96 (2003) 357–366.

[16] V. Brabec, E. Palecek, Interaction of nucleic acids with electrically charged surfaces. II. Conformational changes in double-helical polynucleotides, Biophys. Chem. 4 (1976) 76–92.

[17] V. Brabec, E. Palecek, The influence of salts and pH on polarographic currents produced by denatured DNA, Biophysik 6 (1970) 290–300.

[18] J.H. Murphy, T.L. Trapane, Concentration and extinction coefficient determination for oligonucleotides and analogs using a general phosphate analysis, Anal. Biochem. 240 (1996) 273–282.

[19] N. Poklar, D.S. Pilch, S.J. Lippard, E.A. Redding, S.U. Dunham, K.J. Breslauer, Influence of cisplatin intrastrand crosslinking on the conformation, thermal stability, and energetics of a 20-mer DNA duplex, Proc. Natl. Acad. Sci. U. S. A. 93 (1996) 7606–7611.

[20] C.J. Jones, R.D. Wood, Preferential binding of the xeroderma pigmentosum group A complementing protein to damaged DNA, Biochemistry 32 (1993) 12096–12104.

[21] M. Missura, T. Buterin, R. Hindges, U. Hubscher, J. Kasparkova, V. Brabec, H. Naegeli, Double-check probing of DNA bending and unwinding by XPA–RPA: an architectural function in DNA repair, EMBO J. 20 (2001) 3554–3564.

[22] J. Kasparkova, O. Delalande, M. Stros, M.A. Elizondo-Riojas, M. Vojtiskova, J. Kozelka, V. Brabec, Recognition of DNA interstrand cross-link of antitumor cisplatin by HMGB1 protein, Biochemistry 42 (2003) 1234–1244.

[23] M. Stros, DNA bending by the chromosomal protein HMG1 and its high mobility group box domains. Effect of flanking sequences, J. Biol. Chem. 273 (1998) 10355–10361.

[24] M. Stros, Two mutations of basic residues within the N-terminus of HMG-1 B domain with different effects on DNA supercoiling and binding to bent DNA, Biochemistry 40 (2001) 4769–4779.

[25] J. Kasparkova, K.J. Mellish, Y. Qu, V. Brabec, N. Farrell, Site-specific d(GpG) intrastrand cross-links formed by dinuclear platinum complexes. Bending and NMR studies, Biochemistry 35 (1996) 16705–16713.

[26] V. Brabec, M. Sip, M. Leng, DNA conformational distortion produced by site-specific interstrand cross-link of trans-diamminedichloroplatinum(II), Biochemistry 32 (1993) 11676–11681.

[27] S.A. Leharne, B.Z. Chowdhry, Thermodynamic background to differential scanning calorimetry, in: J.E. Ladbury, B.Z. Chowdhry (Eds.), Biocalorimetry: Applications of Calorimetry in the Biological Sciences, J. Wiley & Sons, Chichester, UK, 1998, pp. 157–182.

[28] C. Hofr, N. Farrell, V. Brabec, Thermodynamic properties of duplex DNA containing a site-specific d(GpG) intrastrand crosslink formed by an antitumor dinuclear platinum complex, Nucleic Acids Res. 29 (2001) 2034–2040.

[29] C. Hofr, V. Brabec, Thermal and thermodynamic properties of duplex DNA containing site-specific interstrand cross-link of antitumor cisplatin or its clinically ineffective trans isomer, J. Biol. Chem. 276 (2001) 9655–9661.

[30] S.F. Bellon, J.H. Coleman, S.J. Lippard, DNA unwinding produced by site-specific intrastrand cross-links of the antitumor drug cis-diamminedichloroplatinum(II), Biochemistry 30 (1991) 8026–8035.

[31] J. Kasparkova, N. Farrell, V. Brabec, Sequence specificity, conformation, and recognition by HMG1 protein of major DNA interstrand cross-links of antitumor dinuclear platinum complexes, J. Biol. Chem. 275 (2000) 15789–15798.

[32] A. Rodger, Linear dichroism, Methods Enzymol. 226 (1993) 232–258.

[33] A. Rodger, B. Norden, Circular Dichroism and Linear Dichroism, Oxford University Press, Oxford, New York, Tokyo, 1997.

[34] J. Malina, J. Kasparkova, G. Natile, V. Brabec, Recognition of major DNA adducts of enantiomeric cisplatin analogs by HMG box proteins and nucleotide excision repair of these adducts, Chem. Biol. 9 (2002) 629–638.

[35] J. Zehnulova, J. Kasparkova, N. Farrell, V. Brabec, Conformation, recognition by high mobility group domain proteins, and nucleotide excision repair of DNA intrastrand cross-links of novel antitumor trinuclear platinum complex BBR3464, J. Biol. Chem. 276 (2001) 22191–22199.

[36] J. Kasparkova, J. Zehnulova, N. Farrell, V. Brabec, DNA interstrand cross-links of the novel antitumor trinuclear platinum complex BBR3464. Conformation, recognition by high mobility group domain proteins, and nucleotide excision repair, J. Biol. Chem. 277 (2002) 48076–48086.

[37] P.E. Nielsen, Chemical and photochemical probing of DNA complexes, J. Mol. Recognit. 3 (1990) 1–24.

[38] J. Malina, C. Hofr, L. Maresca, G. Natile, V. Brabec, DNA interactions of antitumor cisplatin analogs containing enantiomeric amine ligands, Biophys. J. 78 (2000) 2008–2021.

[39] D.S. Pilch, S.U. Dunham, E.R. Jamieson, S.J. Lippard, K.J. Breslauer, DNA sequence context modulates the impact of a cisplatin 1,2-d(GpG) intrastrand cross-link and the conformational and thermodynamic properties of duplex DNA, J. Mol. Biol. 296 (2000) 803–812.

[40] C. Hofr, V. Brabec, Thermal stability and energetics of 15-mer DNA duplex interstrand cross-linked by trans-diamminedichloroplatinum(II), Biopolymers 77 (2005) 222–229.

[41] J. Malina, O. Novakova, M. Vojtiskova, G. Natile, V. Brabec, Conformation of DNA GG intrastrand cross-link of antitumor oxaliplatin and its enantiomeric analog, Biophys. J. 93 (2007) 3950–3962.

[42] V. Bursova, J. Kasparkova, C. Hofr, V. Brabec, Effects of monofunctional adducts of platinum(II) complexes on thermodynamic stability and energetics of DNA duplexes, Biophys. J. 88 (2005) 1207–1214.

[43] D.S. Pilch, G.E. Plum, K.J. Breslauer, The thermodynamics of DNA structures that contain lesions or guanine tetrads, Curr. Opin. Struct. Biol. 5 (1995) 334–342.

[44] G.E. Plum, C.A. Gelfand, K.J. Breslauer, Physicochemical approaches to structural elucidation. Effects of 3, N4-ethenodeoxycytidine on duplex stability and energetics, in: B. Singer, H. Bartsch (Eds.), Exocyclic DNA Adducts in Mutagenesis and Carcinogenesis, Vol. Publications No. 150, International Agency for Research on Cancer, Lyon, 1999, pp. 169–177.

[45] L.A. Marky, K.J. Breslauer, Calculating thermodynamic data for transitions of any molecularity from equilibrium melting curves, Biopolymers 26 (1987) 1601–1620.

[46] K.M. Comess, J.N. Burstyn, J.M. Essigmann, S.J. Lippard, Replication inhibition and translesion synthesis on templates containing site-specifically placed cis-diamminedichloroplatinum(II) DNA adducts, Biochemistry 31 (1992) 3975–3990.

[47] Z. Suo, K. Johnson, DNA secondary structure effects on DNA synthesis catalyzed by HIV-1 reverse transcriptase, J. Biol. Chem. 273 (1998) 27259–27267.

[48] A. Vaisman, M.W. Warren, S.G. Chaney, The effect of DNA structure on the catalytic efficiency and fidelity of human DNA polymerase beta on templates with platinum–DNA adducts, J. Biol. Chem. 276 (2001) 18999–19005.

[49] E. Bassett, A. Vaisman, J.M. Havener, C. Masutani, F. Hanaoka, S.G. Chaney, Efficiency of extension of mismatched primer termini across from cisplatin and oxaliplatin adducts by human DNA polymerases beta and eta in vitro, Biochemistry 42 (2003) 14197–14206.

[50] J. Kasparkova, O. Novakova, V. Marini, Y. Najajreh, D. Gibson, J.-M. Perez, V. Brabec, Activation of trans geometry in bifunctional mononuclear platinum complexes by a piperidine ligand: mechanistic studies on antitumor action, J. Biol. Chem. 278 (2003) 47516–47525.

[51] B. Moriarity, O. Novakova, N. Farrell, V. Brabec, J. Kasparkova, 1,2-GG intrastrand cross-link of antitumor dinuclear bifunctional platinum compound with spermidine linker inhibits DNA polymerization more effectively than the cross-link of conventional cisplatin, Arch. Biochem. Biophys. 459 (2007) 264–272.

[52] A. Alt, K. Lammens, C. Chiocchini, A. Lammens, J.C. Pieck, D. Kuch, K.P. Hopfner, T. Carell, Bypass of DNA lesions generated during anticancer treatment with cisplatin by DNA polymerase, Science 318 (2007) 967–970.

[53] K. Stehlikova, H. Kostrhunova, J. Kasparkova, V. Brabec, DNA bending and unwinding due to the major 1,2-GG intrastrand cross-link formed by antitumor cis-diamminedichloroplatinum(II) are flanking-base independent, Nucleic Acids Res. 30 (2002) 2894–2898.

[54] J.A. Rice, D.M. Crothers, A.L. Pinto, S.J. Lippard, The major adduct of the antitumor drug cis-diamminedichloroplatinum(II) with DNA bends the duplex by ~40° toward the major groove, Proc. Natl. Acad. Sci. U. S. A. 85 (1988) 4158–4161.

[55] S.F. Bellon, S.J. Lippard, Bending studies of DNA site-specifically modified by cisplatin, trans-diamminedichloroplatinum(II) and cis-Pt(NH$_3$)$_2$(N3-cytosine)Cl$^+$, Biophys. Chem. 35 (1990) 179–188.

[56] H.S. Koo, H.M. Wu, D.M. Crothers, DNA bending at adenine–thymine tracts, Nature 320 (1986) 501–506.

[57] M. Kartalou, J.M. Essigmann, Recognition of cisplatin adducts by cellular proteins, Mutat. Res. 478 (2001) 1–21.

[58] Y. Jung, S.J. Lippard, Direct cellular responses to platinum-induced DNA damage, Chem. Rev. 107 (2007) 1387–1407.

[59] J. Kasparkova, O. Novakova, O. Vrana, F. Intini, G. Natile, V. Brabec, Molecular aspects of antitumor effects of a new platinum(IV) drug, Mol. Pharmacol. 70 (2006) 1708–1719.

[60] V. Brabec, K. Stehlikova, J. Malina, M. Vojtiskova, J. Kasparkova, Thermodynamic properties of damaged DNA and its recognition by xeroderma pigmentosum group A protein and replication protein A, Arch. Biochem. Biophys. 446 (2006) 1–10.

[61] N.E. Geacintov, S. Broyde, T. Buterin, H. Naegeli, M. Wu, S.X. Yan, D.J. Patel, Thermodynamic and structural factors in the removal of bulky DNA adducts by the nucleotide excision repair machinery, Biopolymers 65 (2002) 202–210.

[62] J. SantaLucia Jr., A unified view of polymer, dumbbell, and oligonucleotide DNA nearest-neighbor thermodynamics, Proc. Natl. Acad. Sci. U. S. A. 95 (1998) 1460–1465.

[63] A. Rodger, R. Marington, M.A. Geeves, M. Hicks, L. de Alwis, D.J. Halsall, T.R. Dafforn, Looking at long molecules in solution: what happens when they are subjected to Couette flow? Phys. Chem. Chem. Phys. 8 (2006) 3161–3171.

[64] D. Weaver, E. Crawford, K. Warner, F. Elkhairi, S. Khuder, J. Willey, ABCC5, ERCC2, XPA and XRCC1 transcript abundance levels correlate with cisplatin chemoresistance in non-small cell lung cancer cell lines, Mol. Cancer 4 (2005) 18–25.

[65] T. Fujii, S. Toyooka, K. Ichimura, Y. Fujiwara, K. Hotta, J. Soh, H. Suehisa, N. Kobayashi, M. Aoe, T. Yoshino, K. Kiura, H. Date, ERCC1 protein expression predicts the response of cisplatin-based neoadjuvant chemotherapy in non-small-cell lung cancer, Lung Cancer 59 (2008) 377–384.

[66] G.E. Plum, K.J. Breslauer, DNA lesions: a thermodynamic perspective, Ann. N. Y. Acad. Sci. 726 (1994) 45–56.

[67] J. Florian, J. Kasparkova, N. Farrell, V. Brabec, Thermodynamic stability and energetics of DNA duplexes containing major intrastrand cross-links of second-generation antitumor dinuclear Pt^{II} complexes, J. Biol. Inorg. Chem. 17 (2012) 187–196.